Correlation strength with modern nucleon-nucleon potentials in the Brueckner-Hartree-Fock approach

Zeng-Hua Li (李增花)
Institute of Modern Physics, Fudan University, Shanghai 200433, People's Republic of China

H.-J. Schulze
INFN Sezione di Catania, Dipartimento di Fisica, Universitá di Catania, Via Santa Sofia 64, 95123 Catania, Italy
(Received 24 June 2016; published 15 August 2016)

We calculate the correlation parameter κ of symmetric nuclear matter in the Brueckner-Hartree-Fock approximation obtained with various modern nucleon-nucleon potentials of high precision. We point out qualitative differences between the potentials and elucidate the consequences for momentum distributions, defect functions, and convergence of the hole-line expansion. The important role of the tensor force is emphasized.

DOI: 10.1103/PhysRevC.94.024322

I. INTRODUCTION

The Brueckner-Hartree-Fock (BHF) approach [1], or more generally the underlying Brueckner-Bethe-Goldstone (BBG) formalism, is a well-proven method for the calculation of various properties of nuclear matter, even up to supranuclear densities relevant for astrophysical applications [2]. The only required input is a nonrelativistic nucleon-nucleon (NN) potential fitted to scattering data. With the time, more and more precise meson-exchange NN potentials have become available [3–8] and this trend continues with the recent development of potentials in the framework of chiral perturbation theory [9,10].

An important parameter in the BBG formalism is the "correlation strength" κ, sometimes called "depletion parameter" or "wound integral." It characterizes the strength of NN correlations generated by the NN interaction, and plays a significant role in understanding the structure of finite nuclei and neutron star physics. Recent experimental measurements provided evidence for the existence of short-range correlations in balanced and imbalanced Fermi systems [11]. Theoretically, this effect is expected to be derived from the nuclear "hard core" and the tensor part in the NN potentials [12–15].

The correlation strength parameter κ is related to several physical quantities such as the momentum distribution, the spectral function, or the defect function, and is believed to be an indicator for the convergence of the so-called BBG hole-line expansion [1,16]. Previously, a close connection between the correlation parameter and the saturation properties of nuclear matter in the BHF approximation has been pointed out [17], and the purpose of our current work is to present updated results for momentum distributions, defect functions, and correlation parameter for modern NN potentials that fit the NN phase shifts with high precision. In particular, we consider the Paris [3], Nijmegen 93 [6], Argonne V18 [7], Bonn B [5], and CDBonn [8] potentials, as well as the recent N3LO chiral potentials [9] with two values of the chiral cutoff $\Lambda = 450, 500$ MeV. We will analyze the important qualitative differences between these potentials.

We work here entirely in the lowest-order BHF approximation, since in fact the corrections to those results are thought to be controlled by the correlation parameter. We also restrict this study to symmetric nuclear matter.

II. FORMALISM AND RESULTS

We recall that the nucleon momentum distribution in BHF approximation can be obtained as [18–22]

$$n(k < k_F) = 1 + \left.\frac{\partial M_1(k,\omega)}{\partial\omega}\right|_{\omega=e_k}, \tag{1}$$

$$n(k > k_F) = -\left.\frac{\partial M_2(k,\omega)}{\partial\omega}\right|_{\omega=e_k}, \tag{2}$$

where

$$M_1(1,\omega) = \sum_{2<k_F} \langle 12|G(\omega+e_2)|12\rangle_A, \tag{3}$$

$$M_2(1,\omega) = \frac{1}{2}\sum_{\substack{3,4<k_F\\2>k_F}} \frac{\left|\langle 12|G(e_3+e_4)|34\rangle_A\right|^2}{\omega+e_2-e_3-e_4-i\delta} \times (2\pi)^3\delta^3(\boldsymbol{k}_1+\boldsymbol{k}_2-\boldsymbol{k}_3-\boldsymbol{k}_4) \tag{4}$$

are the direct and rearrangement contributions to the single-particle (s.p.) mass operator or self-energy, and

$$e_k = \frac{k^2}{2m} + \mathrm{Re}\, M_1(k,e_k) \tag{5}$$

is the on-shell s.p. energy in the continuous-choice BHF approximation. We have introduced multi-indices for the nucleon degrees of freedom $1 \equiv (s,t,\boldsymbol{k})_1$ etc., such that the total density of symmetric nuclear matter is

$$\rho = \sum_{1<k_F} = 4\int_0^{k_F} \frac{d^3\boldsymbol{k}}{(2\pi)^3} = \frac{2k_F^3}{3\pi^2}. \tag{6}$$

One can then define the depletion parameter

$$\kappa \equiv \sum_k n(k>k_F) \Big/ \sum_{k<k_F}, \tag{7}$$

which measures the "correlatedness" of the interacting system in the sense of finding a nucleon scattered out of the

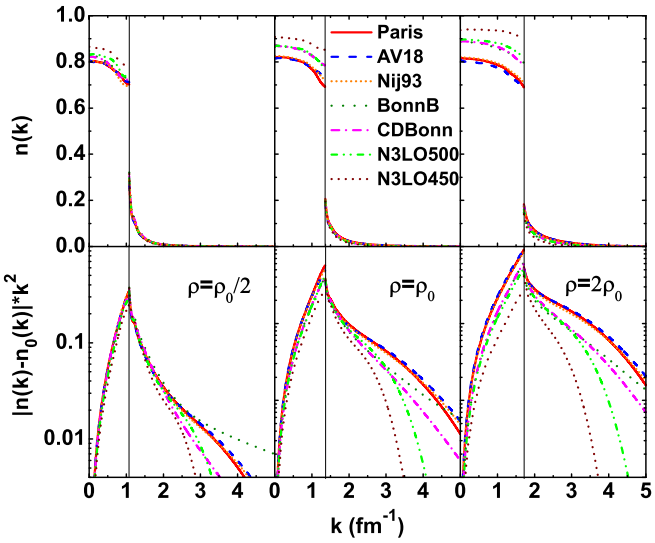

FIG. 1. Top panel: Momentum distributions $n(k)$ at different densities ($\rho_0 = 0.17$ fm^{-3}) for different potentials. Bottom panel: The weighted deviations from the bare Fermi distribution $n_0(k) = \theta(k_F - k)$.

unperturbed ground state of a free Fermi gas with momentum distribution $n_0(k) = \theta(k_F - k)$.

As a first illustration, we plot in Fig. 1 the momentum distributions obtained with different NN potentials at three different densities $\rho = 0.085, 0.17, 0.34$ fm^{-3}, and in the upper panel of Fig. 2 the corresponding depletion parameter κ

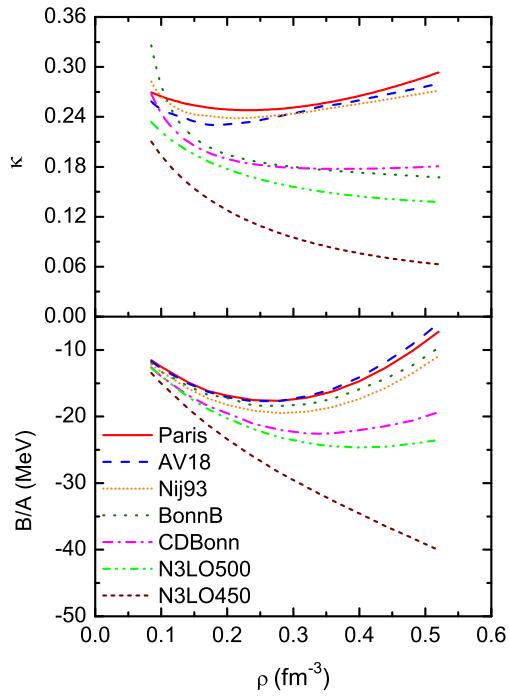

FIG. 2. Top panel: Average depletion of the momentum distribution, Eq. (7), as a function of density for different potentials. Bottom panel: Saturation curves of symmetric nuclear matter in the BHF approximation for different potentials.

as a function of density. One notes immediately substantial quantitative differences between the different potentials, in particular at high density, $\rho \gtrsim \rho_0 = 0.17$ fm^{-3}, where the depletion for the r-space potentials Paris, V18, Nij93 remains fairly high, whereas the k-space and in particular the chiral potentials feature much lower values. In the latter case, there is a strong dependence on the chiral cutoff. The conclusion is that the depletion at high density is determined by the repulsive core of the NN interaction, which is very strong in the r-space potentials and very weak in the chiral potentials with small cutoff.

Also the saturation curves of nuclear matter, shown in the lower panel of Fig. 2, depend decisively on the strength of the nuclear core. One observes in fact a very clear correlation between the density dependence of κ and B/A. In both cases, the density dependence is related to the one of the G matrix in the Bethe-Goldstone equation,

$$G = V - V\frac{Q}{E - W}G, \tag{8}$$

caused by the Pauli operator Q (Pauli quenching of the effective interaction) and by the starting energy W (dispersive quenching) [12,23]. "Hard" potentials with a strong tensor force feature larger contributions of second and higher order in V on the right-hand side of Eq. (8), and thus the G matrix becomes less attractive at high density due to the quenching effects.

We note in particular that the "weakest," chiral potentials saturate only at very large density and too much binding energy, or not at all. At the same time, however, the correlation parameter becomes very small, such that any corrections to the saturation curve in the hole-line expansion are also expected to be small. Therefore, as is well known [24], the only way to achieve realistic saturation properties with the "weak" potentials is the inclusion of very strong three-nucleon (or higher-order) forces.

In order to analyze in more detail the density dependence of κ, we now establish a link to the NN defect functions in the different partial waves. Defining

$$F(1,2,3,4) \equiv \frac{1}{2}\left|\frac{\langle 12|G(e_3+e_4)|34\rangle_A}{e_1+e_2-e_3-e_4}\right|^2 \tag{9}$$

and

$$\sum_{\substack{3,4<k_F\\1,2>k_F}} = \sum_{1,2} Q_{12} \sum_{3,4} R_{34}, \tag{10}$$

where Q_{12} and R_{34} are the appropriate Pauli and anti-Pauli operators, respectively, one can write Eq. (7) as

$$\kappa = \sum_{1,2} Q_{12} \sum_{3,4} R_{34}\,(2\pi)^3\delta^3(\boldsymbol{p}' - \boldsymbol{p})F(1,2,3,4) \Big/ \sum_{4<k_F}, \tag{11}$$

where we define the total and relative momenta

$$\boldsymbol{p}' = \boldsymbol{k}_1 + \boldsymbol{k}_2, \quad \boldsymbol{q}' = (\boldsymbol{k}_1 - \boldsymbol{k}_2)/2, \tag{12a}$$

$$\boldsymbol{p} = \boldsymbol{k}_3 + \boldsymbol{k}_4, \quad \boldsymbol{q} = (\boldsymbol{k}_3 - \boldsymbol{k}_4)/2. \tag{12b}$$

Performing now suitable phase space averages for the nucleons in the Fermi sea, $3,4 \to \bar{3},\bar{4}$, we obtain

$$\kappa \approx \left[\sum_{3,4} R_{34}\right] \sum_{1,2} Q_{12}(2\pi)^3\delta^3(\boldsymbol{p}' - \bar{\boldsymbol{p}})F(1,2,\bar{3},\bar{4}) \Big/ \sum_{4<k_F} \tag{13}$$

$$= \rho \sum_{1,2} Q_{12}(2\pi)^3\delta^3(\boldsymbol{p}' - \bar{\boldsymbol{p}})F(1,2,\bar{3},\bar{4}), \tag{14}$$

and employing

$$\int d^3\boldsymbol{k}_1 \int d^3\boldsymbol{k}_2 = \int d^3\boldsymbol{p}' \int d^3\boldsymbol{q}' \tag{15}$$

together with an expansion of the G matrix in terms of partial waves $\alpha \equiv (TSJLL')$, the final result is [17]

$$\kappa \approx \sum_{\alpha} \frac{(2T+1)(2J+1)}{8} \rho \int \frac{d^3\boldsymbol{q}'}{(2\pi)^3} Q(\bar{p},q') \left|\frac{G_\alpha(\bar{p},\bar{q},q')}{E(\bar{p},\bar{q},q')}\right|^2, \tag{16}$$

where

$$G_\alpha(\bar{p},\bar{q},q') = 4\pi \int dr\, r^2 j_\alpha(q'r) V_\alpha(r) u_\alpha(r), \tag{17}$$

$$E(\bar{p},\bar{q},q') = E_{12}(\bar{p},q') - E_{34}(\bar{p},\bar{q}) > 0, \tag{18}$$

$$Q(\bar{p},q') = \max\left[0, \min\left[\frac{\bar{p}^2/4 + q'^2 - k_F^2}{\bar{p}q'}, 1\right]\right] \tag{19}$$

are the G-matrix partial-wave elements and the angle-averaged energy denominator and Pauli operator [25], evaluated for averaged initial total and relative momenta in the Fermi sea,

$$\bar{p}^2 = \frac{6}{5}k_F^2, \quad \bar{q}^2 = \frac{3}{10}k_F^2. \tag{20}$$

Assuming finally $Q^2 \approx Q$ for the angle-averaged Pauli-operator Eq. (19), one can establish the relation to the defect functions in momentum space,

$$\eta_\alpha(\bar{p},\bar{q},q') \equiv \frac{Q(\bar{p},q')G_\alpha(\bar{p},\bar{q},q')}{E(\bar{p},\bar{q},q')} \tag{21}$$

and after a Fourier transform to coordinate space,

$$\eta_\alpha(\bar{p},\bar{q},r) = \frac{1}{2\pi^2}\int dq\, q^2 j_\alpha(qr)\eta_\alpha(\bar{p},\bar{q},q), \tag{22}$$

one obtains

$$\kappa \approx \sum_{\alpha} \frac{(2T+1)(2J+1)}{8} \rho \int d^3\boldsymbol{r}\, |\eta_\alpha(\bar{p},\bar{q},r)|^2. \tag{23}$$

This equation relates the correlation parameter κ defined as the average depletion of the momentum distribution to the defect functions η (or correlated wave functions u) in coordinate space,

$$\eta_{LL'}(r) \equiv j_L(\bar{q}r)\delta_{LL'} - u_{LL'}(r) = \int \frac{d^3\boldsymbol{r}'d^3\boldsymbol{q}'}{(2\pi)^3} \sum_{L''} \times \frac{j_{L'}(q'r)j_{L'}(q'r')Q(q')V_{L'L''}(r')u_{LL''}(r')}{E(q')}, \tag{24}$$

where $\eta_{LL'}$, $u_{LL'}$, Q, E depend implicitly on $\bar{p},\bar{q}$.

Formally Eq. (23) can be written as [16,26]

$$\kappa = \rho \int d^3\boldsymbol{r} \langle|\eta(\boldsymbol{r})|^2\rangle_{S,T} = N\frac{V_{\rm core}}{V} = \left(\frac{c}{d}\right)^3 \tag{25}$$

and expresses the correlation parameter as the ratio of the core (or "wound") volume to the volume per particle, or equivalently, the cubed ratio of core diameter c to average nucleon distance d. Since the core volume or diameter defined in this way from the density-dependent defect functions are not constant, but in general shrink with increasing density, the result is a nonlinear density dependence of the correlation parameter κ, as shown in Fig. 2 (top), that we will analyze in more detail in the following.

Equation (25) has the following interpretation as foundation of the hole-line expansion: For a system with interaction range c and average particle distance $d > c$, the probability of finding a cluster of n interacting (correlated) particles is $(c/d)^{3n} = \kappa^n \ll 1$. This suggests grouping the energy diagrams according to the number of interacting particles; first two-body correlations or clusters, then three-body correlations, etc. The number of interacting particles is equivalent to the number of hole lines, so this leads to the hole-line expansion,

$$B/A = (T + E_2 + E_3 + \cdots)/A, \tag{26}$$

which amounts to an expansion in density governed by the dimensionless parameter $\kappa = \rho V_{\rm core}$. However, this assertion obviously hinges on the condition that the dominant component of the interaction is the short-range core part, and therefore in practice the convergence of the hole-line expansion should be verified for any potential by explicit computation [27], which is an arduous task.

Due to the numerous approximations and averages in order to reduce the number of integrations from 4×3 in Eq. (11) to 1 in Eq. (23), the latter equation is not exact, but we will use it now to study explicitly the different partial-wave contributions to the right-hand side.

As an illustration [28] we show in Fig. 3 the r-space defect functions in the $^1S_0$ and $^3SD_1$ partial waves, $\eta_{^1S_0}(r)$ and $\eta_{^3SD_1}(r)$, at various densities and for different potentials. One observes clearly the different characteristics of the potentials mentioned before: The r-space potentials are very "hard," with a large "defect" at small distance, while the chiral potentials are very "soft." Apart from the extremely soft N3LO450 potential, the density dependence (quenching) regards mainly the medium- and long-range ($r \gtrsim 1$ fm) behavior, thus the hard core persists up to large density and the density dependence is much stronger for the long-range $^3SD_1$ wave. This wave is directly generated by the tensor force, and in this coupled channel the defect function coincides with the correlated wave function that is

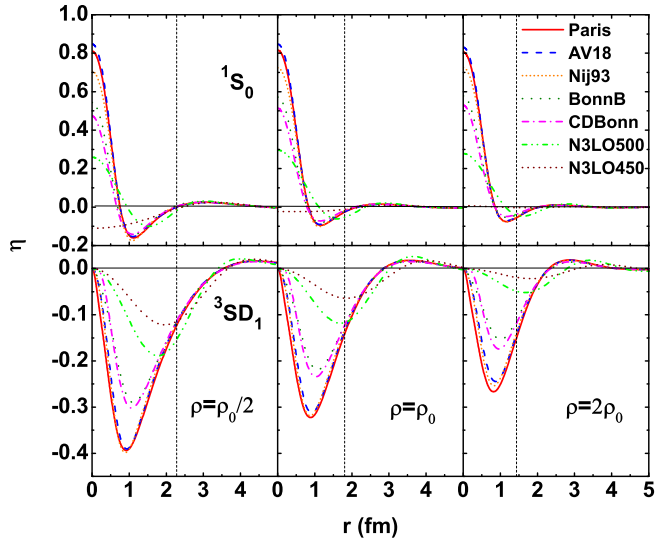

FIG. 3. $^1S_0$ (upper panels) and $^3SD_1$ (lower panels) defect functions at different densities ($\rho_0 = 0.17$ fm^{-3}) for different potentials. The vertical dashed lines indicate the interparticle distance $d \equiv \rho^{-1/3}$.

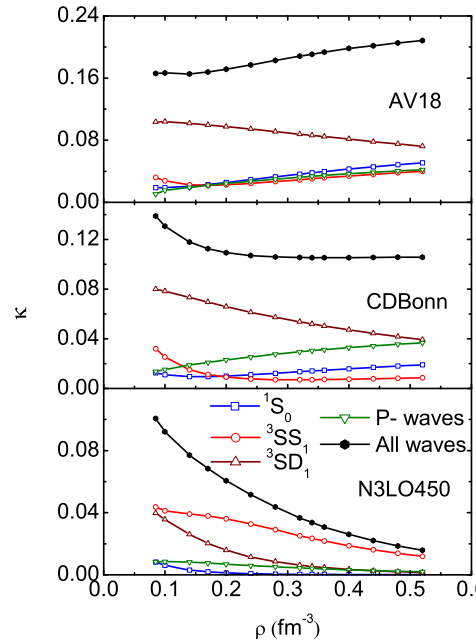

FIG. 4. Partial-wave contributions to the correlation parameter for the V18 (upper panel), CDBonn (central panel), and N3LO450 (lower panel) potentials.

responsible for the deuteron bound state at very low density. The vertical dashed lines in the figure indicate a typical interparticle distance $d \equiv \rho^{-1/3}$, and one can clearly see that the hole-line expansion condition $c < d$ is well fulfilled for the short-range $^1S_0$, but not for the $^3SD_1$ wave, in particular for the chiral potentials.

Also in this regard, our last point of interest concerns the relative contributions of the different partial waves to the total value of the correlation parameter, and this is addressed in Fig. 4, where we plot separately the contributions of the s waves $^1S_0$, $^3SS_1$, $^3SD_1$, and the sum of the p waves $^1P_1$ and $^3P_{0,1,2}$. Higher partial waves practically play no role over the whole density range considered. We compare a typical "hard" potential, V18, (upper panel) with an intermediate one, CD-Bonn, (central panel), and a very soft one, N3LO450, (lower panel). An essential feature of any realistic NN potential is the necessity of a strong tensor force, and consequently the coupled $^3SD_1$ partial wave provides the largest contribution to many physical observables. This is also the case here, and in the partial wave summation of Eq. (23) the largest contributor is $|\eta_{SS}|^2 + |\eta_{SD}|^2$,$(T = 0, S = 1)$, namely the deuteron channel [15].

In the case of the V18 potential (top panel), the $^3SD_1$ channel provides by far the most important contribution to κ around normal nuclear density, but its value decreases with increasing density, according to the density-dependent suppression observed in Fig. 3. This might be attributed to the in-medium screening of the deuteron bound state in dense nuclear matter [29]. On the other hand, the remaining partial-wave contributions increase nearly linear with increasing density, which means that the excluded "hard-core" volume $V_{\rm core}$ remains nearly independent of density, see Fig. 3 (top), and the linear increase of κ_α is caused by the factor ρ in Eqs. (23) and (25).

The behavior of the extremely "soft" N3LO450 potential (bottom panel) is completely different due to the absence of a hard core: The correlation volume in Fig. 3 strongly decreases with density, and so do all partial-wave contributions to κ. The CDBonn potential (central panel) features intermediate characteristics: the p-wave contributions still increase with density, but the $^3SS_1$ does not.

Thus the competition between the long-range $^3SD_1$ deuteron partial wave and the other more short-range channels determines the overall density dependence of the correlation strength κ for the different potentials. For soft potentials all correlation volumes and even the parameters κ_α disappear fast with increasing density, whereas for hard potentials the correlation strength might increase again with density due to the dominance of the persistent p-wave contributions at high density. For very hard potentials with constant $V_{\rm core} = 4\pi r^3/3$; $r \approx d/2 \approx 0.4$ fm in Eq. (25), one obtains $\kappa \approx 0.3$ fm$^3 \times \rho$, which is approximately fulfilled for $\kappa - \kappa_{^3SD_1}$ at large density in Fig. 4 (top).

The total values of κ reported in Fig. 4 are somewhat smaller than those in Fig. 2. This is mainly due to the fact that for the angle-averaged Pauli operator $Q^2 < Q$, and not $Q^2 = Q$ as for the exact Pauli operator, which was assumed when going from Eq. (16) to Eq. (23). The agreement could be improved by using $\sqrt{Q}$ instead of Q in Eq. (21). However, the qualitative conclusions are not affected by this approximation.

III. CONCLUSIONS

We have examined the correlation strength of various modern NN potentials and pointed out the connection to momentum distributions and defect functions. We found qualitatively different behaviors for "hard" and "soft" potentials related to the competition between short-range and long-range components, and in particular very low κ values for chiral

potentials with small cutoff. This implies that in this case the hole-line expansion is well converged already at BHF level, and that very strong nuclear three-body forces are required in order to achieve satisfactory saturation properties of nuclear matter. On the other hand, for these very soft potentials, the condition of a dominant short-range component of the interaction that is the foundation of the hole-line expansion, might be violated. Therefore, an important task for the future is to quantitatively confirm this conjecture by computing explicitly the three-hole-line contributions to the binding energy for these potentials.

ACKNOWLEDGMENTS

We acknowledge useful discussions with M. Baldo. This work is sponsored by the National Natural Science Foundation of China under Grants No. 11075037 and No. 11475045, the Scientific Research Foundation for the Returned Overseas Chinese Scholars, State Education Ministry, the Fundamental Research Funds for the Central Universities of China, and the Shanghai Leading Academic Discipline Project (B107). We further acknowledge partial support from "NewCompStar," COST Action MP1304.

[1] K. A. Brueckner and J. L. Gammel, Phys. Rev. **109**, 1023 (1958); J. P. Jeukenne, A. Lejeune, and C. Mahaux, Phys. Rep. **25**, 83 (1976); B. Day, Nucl. Phys. A **328**, 1 (1979); M. Baldo, *Nuclear Methods and the Nuclear Equation of State*, International Review of Nuclear Physics, Vol. 8 (World Scientific, Singapore, 1999); M. Baldo and G. F. Burgio, Rep. Prog. Phys. **75**, 026301 (2012).

[2] M. Baldo, I. Bombaci, and G. F. Burgio, Astron. Astrophys. **328**, 274 (1997); X. R. Zhou, G. F. Burgio, U. Lombardo, H.-J. Schulze, and W. Zuo, Phys. Rev. C **69**, 018801 (2004); Z. H. Li and H.-J. Schulze, *ibid.* **78**, 028801 (2008).

[3] M. Lacombe, B. Loiseau, J. M. Richard, R. Vinh Mau, J. Côté, P. Pirés, and R. de Tourreil, Phys. Rev. C **21**, 861 (1980).

[4] R. B. Wiringa, R. A. Smith, and T. L. Ainsworth, Phys. Rev. C **29**, 1207 (1984).

[5] R. Machleidt, K. Holinde, and Ch. Elster, Phys. Rep. **149**, 1 (1987).

[6] V. G. J. Stoks, R. A. M. Klomp, C. P. F. Terheggen, and J. J. de Swart, Phys. Rev. C **49**, 2950 (1994).

[7] R. B. Wiringa, V. G. J. Stoks, and R. Schiavilla, Phys. Rev. C **51**, 38 (1995).

[8] R. Machleidt, Phys. Rev. C **63**, 024001 (2001).

[9] D. R. Entem and R. Machleidt, Phys. Lett. B **524**, 93 (2002); Phys. Rev. C **68**, 041001(R) (2003); D. R. Entem, N. Kaiser, R. Machleidt, and Y. Nosyk, *ibid.* **92**, 064001 (2015).

[10] E. Epelbaum, W. Glöckle, and U.-G. Meissner, Nucl. Phys. A **747**, 362 (2005); E. Epelbaum, H. Krebs, and U.-G. Meissner, Eur. Phys. J. A **51**, 53 (2015).

[11] R. Subedi *et al.*, Science **320**, 1476 (2008); O. Hen *et al.*, *ibid.* **346**, 614 (2014).

[12] H. Müther and A. Polls, Prog. Part. Nucl. Phys. **45**, 243 (2000).

[13] W. H. Dickhoff and C. Barbieri, Prog. Part. Nucl. Phys. **52**, 377 (2004); H. Müther and I. Sick, Phys. Rev. C **70**, 041301(R) (2004).

[14] M. M. Sargsian, T. V. Abrahamyan, M. I. Strikman, and L. L. Frankfurt, Phys. Rev. C **71**, 044614 (2005); **71**, 044615 (2005); R. Schiavilla, R. B. Wiringa, S. C. Pieper, and J. Carlson, Phys. Rev. Lett. **98**, 132501 (2007).

[15] A. Rios, A. Polls, and W. H. Dickhoff, Phys. Rev. C **79**, 064308 (2009); **89**, 044303 (2014).

[16] H. A. Bethe, B. H. Brandow, and A. G. Petschek, Phys. Rev. **129**, 225 (1963); B. H. Brandow, *ibid.* **152**, 863 (1966); M. W. Kirson, Nucl. Phys. A **99**, 353 (1967); B. D. Day, Rev. Mod. Phys. **39**, 719 (1967); R. Rajaraman and H. A. Bethe, *ibid.* **39**, 745 (1967).

[17] M. I. Haftel and F. Tabakin, Nucl. Phys. A **158**, 1 (1970); Phys. Rev. C **3**, 921 (1971); F. Coester, S. Cohen, B. Day, and C. M. Vincent, *ibid.* **1**, 769 (1970); B. D. Day and F. Coester, *ibid.* **13**, 1720 (1976).

[18] P. Grange, J. Cugnon, and A. Lejeune, Nucl. Phys. A **473**, 365 (1987).

[19] M. Baldo, I. Bombaci, L. S. Ferreira, G. Giansiracusa, and U. Lombardo, Phys. Lett. B **209**, 135 (1988); M. Baldo, I. Bombaci, G. Giansiracusa, and U. Lombardo, Nucl. Phys. A **530**, 135 (1991); M. Baldo, I. Bombaci, G. Giansiracusa, U. Lombardo, C. Mahaux, and R. Sartor, *ibid.* **545**, 741 (1992).

[20] A. Ramos, W. H. Dickhoff, and A. Polls, Phys. Rev. C **43**, 2239 (1991).

[21] M. Baldo, M. Borromeo, and C. Ciofi degli Atti, Nucl. Phys. A **604**, 429 (1996).

[22] W. Zuo, I. Bombaci, and U. Lombardo, Phys. Rev. C **60**, 024605 (1999); P. Yin, J.-Y. Li, P. Wang, and W. Zuo, *ibid.* **87**, 014314 (2013); P. Wang, S.-X. Gan, P. Yin, and W. Zuo, *ibid.* **87**, 014328 (2013); P. Wang and W. Zuo, *ibid.* **89**, 054319 (2014).

[23] H. Müther and P. U. Sauer, in *Computational Nuclear Physics 2: Nuclear Reactions*, edited by K. Langanke, J. A. Maruhn, and S. E. Koonin (Springer, New York, 1993).

[24] K. Hebeler, S. K. Bogner, R. J. Furnstahl, A. Nogga, and A. Schwenk, Phys. Rev. C **83**, 031301(R) (2011); Z. H. Li and H.-J. Schulze, *ibid.*, **85**, 064002 (2012); L. Coraggio, J. W. Holt, N. Itaco, R. Machleidt, L. E. Marcucci, and F. Sammarruca, *ibid.* **89**, 044321 (2014); F. Sammarruca, L. Coraggio, J. W. Holt, N. Itaco, R. Machleidt, and L. E. Marcucci, *ibid.* **91**, 054311 (2015); A. Carbone, A. Rios, and A. Polls, *ibid.* **90**, 054322 (2014); D. Logoteta, I. Vidaña, I. Bombaci, and A. Kievsky, *ibid.* **91**, 064001 (2015); M. Kohno, Prog. Theor. Exp. Phys. 123D02 (2015); D. Logoteta, I. Bombaci, and A. Kievsky, Phys. Lett. B **758**, 449 (2016).

[25] H.-J. Schulze, A. Schnell, G. Röpke, and U. Lombardo, Phys. Rev. C **55**, 3006 (1997); H.-J. Schulze, M. Baldo, U. Lombardo, J. Cugnon, and A. Lejeune, *ibid.* **57**, 704 (1998).

[26] M. Baldo and H. R. Moshfegh, Phys. Rev. C **86**, 024306 (2012).

[27] B. D. Day, Phys. Rev. C **24**, 1203 (1981); H. Q. Song, M. Baldo, G. Giansiracusa, and U. Lombardo, Phys. Rev. Lett. **81**, 1584 (1998); M. Baldo, A. Fiasconaro, H. Q. Song, G. Giansiracusa, and U. Lombardo, Phys. Rev. C **65**, 017303 (2001); M. Baldo and C. Maieron, *ibid.* **72**, 034005 (2005); R. Sartor, *ibid.* **73**, 034307 (2006); M. Baldo, A. Polls, A. Rios, H.-J. Schulze, and I. Vidaña, *ibid.* **86**, 064001 (2012); K. Fukukawa, M. Baldo, G. F. Burgio, L. Lo Monaco, and H.-J. Schulze, *ibid.* **92**, 065802 (2015).

[28] H. Müther and A. Polls, Phys. Rev. C **61**, 014304 (1999); F. Sammarruca, *ibid.* **90**, 064312 (2014).

[29] U. Lombardo, P. Nozières, P. Schuck, H.-J. Schulze, and A. Sedrakian, Phys. Rev. C **64**, 064314 (2001).